

# **Procoagulant Microparticle Interactions due to P-sel-Ig in Hemophilia A Patients**

BEE 4530

Computer-Aided Engineering: Applications to Biomedical Processes

May 11, 2016

Iris Lin  
Gavisha Waidyaratne  
Masoom Chainani  
Ethan Venosa

**Table of Contents**

<b>1. Executive Summary</b> .....	2
<b>2. Introduction</b> .....	3
<b>3. Problem Statement</b> .....	4
<b>4. Process Dynamics</b> .....	5
<b>5. Design Objectives</b> .....	6
<b>6. Governing Equations</b> .....	6
<b>7. Boundary Conditions</b> .....	7
<b>8. Initial Conditions</b> .....	8
<b>9. Results</b> .....	8
<b>10. Sensitivity Analysis</b> .....	11
<b>11. Accuracy Check</b> .....	15
<b>12. Discussion</b> .....	15
<b>13. Appendix</b> .....	18
<b>14. References</b> .....	19

## **Executive Summary**

Congenital hemophilia is a hereditary, X-linked blood-clotting disease that involves insufficient clotting factors VIII and IX. There are two types of hemophilia, Hemophilia A and Hemophilia B. Hemophilia A is the most common form of hemophilia affecting individuals. Current treatment options include recombinant or concentrated plasma procoagulant. However, immunity to these treatment options as well as high treatment cost is common. This research models a treatment option involving P-selectin. P-selectin is a known precursor to tissue clotting factors already present in the body, and therefore can minimize the issue of immunity to treatment. The purpose of this research is to optimize the delivery of a P-selectin precursor in order to minimize clotting time and reduce immunity to drug therapy for hemophilia patients.

In order to simulate this treatment, the drug P-sel-Ig was assumed to have been injected and reacted within the vein to produce an initial steady-state microparticle concentration. In COMSOL, as mass transport through a cylindrical vessel with fluid flow. This model measures the time it takes to accumulate enough fibrin to fully clot the wound. The model also optimizes microparticle concentration to minimize the time taken to clot the wound. The model can be adjusted for varying wound size, location, and time of formation.

This model was validated in optimizing microparticle concentration for promoting the clotting of wounds. The literature value for wound clotting time is approximately 4.5 minutes. In order to achieve a complete wound clot, the clotting time from the model was approximately 35 minutes, which is within an order of magnitude from the literature value. This research defines clotting time as the number of minutes necessary to reach a 90% threshold fibrin density packing ratio. The optimal initial microparticle concentration was  $2.66 \times 10^{-5} \text{ mol/m}^3$ . In addition, the model showed that as wound size increases, the time necessary to close the wound also increases. The computation model demonstrated a range of initial microparticle concentrations necessary to provide adequate fibrin clot formation in response to the wound.

The results of this model can potentially be used in optimizing the design of a regularly administered drug therapy for hemophilia patients to facilitate efficient clotting. This drug therapy would be cheaper treatment option because of its longer half-life. It would also prevent the formation of antibodies, which reduces the effectiveness of current treatment options.

## **Introduction**

Hemophilia is an X-linked, genetic blood-clotting disorder in which individuals are lacking in factor VIII or factor IX [1]. Approximately 400 births per year, and 1 in 5,000 male birth per year, are affected with hemophilia. Based on data and expected births and deaths from 1994, approximately 20,000 people in the United States suffer from hemophilia [2] Individuals with lower than normal levels of factor VIII are considered to have hemophilia A, whereas people lacking factor IX are considered to have hemophilia B. Because of the X-linked inheritance of the disease, majority of hemophilia sufferers are male. Women hemophilia carriers generally have half the concentration of factor VIII and factor IX compared to normal, which is adequate for stable hemostasis. Compared to hemophilia B, hemophilia A is more common in America. There are two types of hemophilia, congenital and acquired. People with congenital hemophilia inherit it from the parents. However, people with acquired hemophilia developed autoantibodies to plasma procoagulants [3].

There are various treatments used currently to treat hemophilia A. They include porcine factor VIII (or other plasma procoagulant concentrates) and recombinant plasma procoagulant. Transfusion with recombinant plasma procoagulant is the most common treatment for hemophilia today [4]. However, it has been shown that people undergoing replacement therapy have developed inhibitors to the transfused procoagulant proteins [5]. Other treatments include injection of plasma concentrates to individuals, essentially treating patients with effective replacement therapy. However, these concentrates can expose patients to alloantigens and viral diseases in the transfusion, such as HIV, hepatitis C, hepatitis B, and delta hepatitis. With issues in current treatments for hemophilia, new therapy options should be developed [4]. In the article by Hrachovinová et al., a new possible treatment option is studied, specifically the generation of procoagulant microparticles from P-selectin binding to P-selectin glycoprotein ligand 1 (PSGL-1), which is necessary for blood clotting and procoagulant activity. This treatment is preferable to current treatments because of the longer half-life (which can allow for an overall cheaper product) and the prevention of antibody formation, which plagues current treatment options.

In this study, doses of P-sel-Ig was injected and binded with endothelial cells in the basilic vein. This process started a pathway which results in the p-selectin formation. P-selectin then binds to PSGL-1, which are present on leukocytes. Binding to leukocytes allowed for the creation of microparticles. Microparticles have tissue-factor, which bound to and activated Factor X. Activated factor X cleaved prothrombin to activated thrombin, which converted fibrinogen to fibrin. Fibrin was directly clotted the wound. In hemophilia patients, this pathway is key to allow for proper clotting of wounds. Therefore, this proposal seeked to understand and optimize the process post P-sel-Ig injection, specifically from steady-state microparticle concentration to blood clotting activity by using a mass transfer model in COMSOL [7].

### **Problem Statement**

One new type of treatments for Hemophilia A patients are P-sel-Ig injections, which induce coagulant microparticle generation. This in turn improves the kinetics of fibrin formation at the sites of bleeding. The circulatory system comes into play because there will be a loss of microparticles from organs, such as the liver and kidneys. The experimental approach to understand the process of microparticles in blood clotting involves calculating the time for the wound to clot once the drug has been circulating within the patient. The calculation of clotting time could also be used to optimize concentration of the drug.

In order to create an appropriate model for this hemophilia treatment, certain aspects are addressed. Specifically, mass transfer of the microparticles in the bloodstream (including calculations through the circulatory system), fluid flow of the blood, and reaction of the microparticles with coagulation factors in the blood to form fibrin will be modeled. COMSOL will be used to model these three steps.

### **Problem Schematic**

This model focuses on drug transport in the right arm basilic vein with a wound area at its end, shown below in Figure 1.

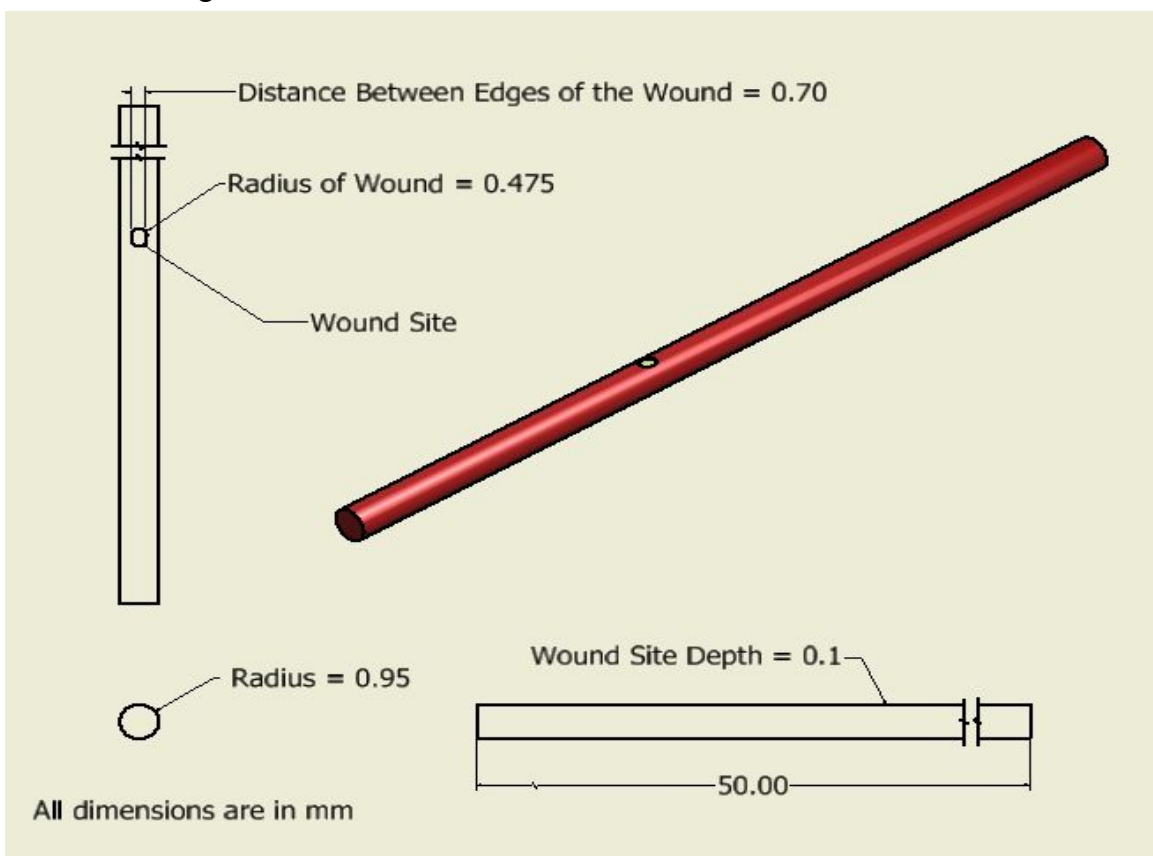
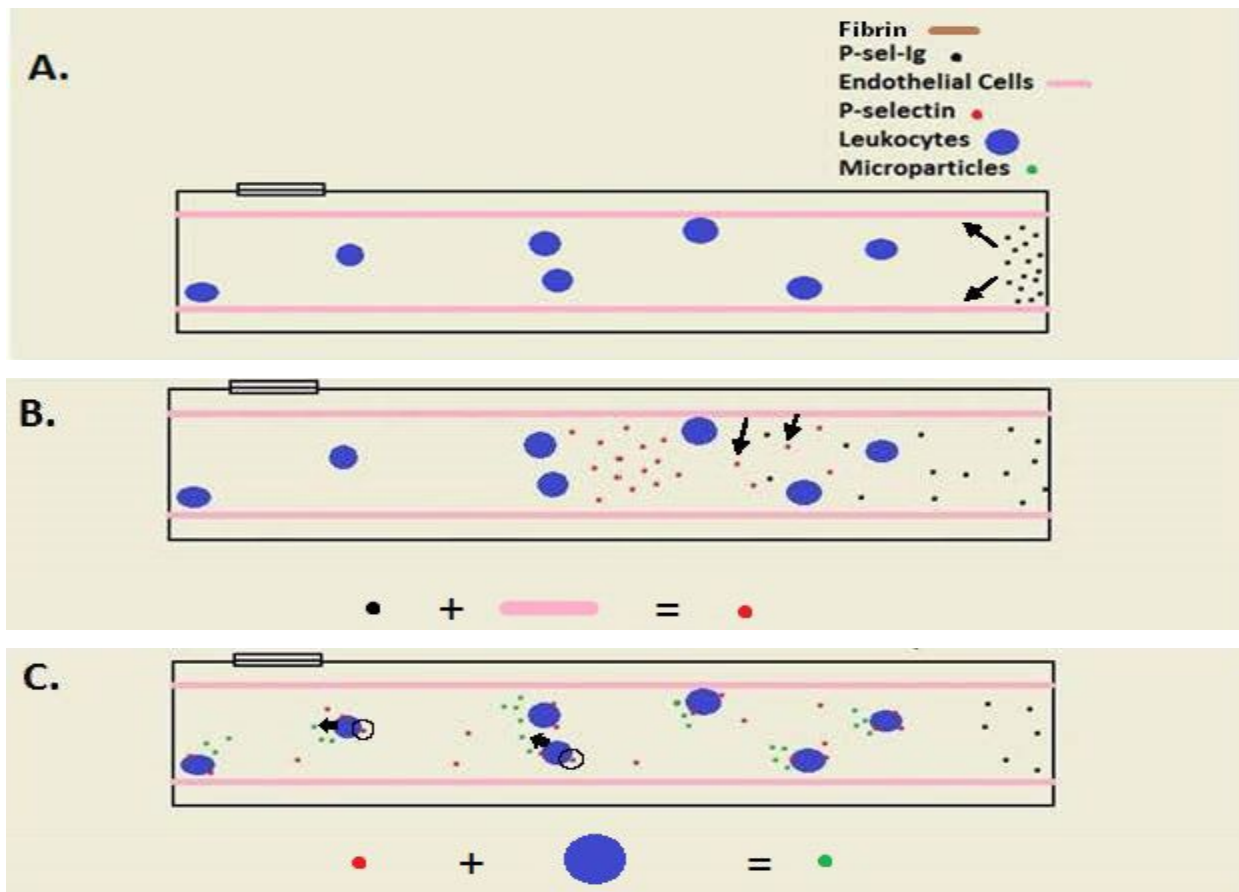


**Figure 1. A schematic of the right arm basilic vein.** The basilic vein [2] is a vessel which runs along the back of the forearm and then passes below the elbow before moving up the middle of the upper arm. It then merges with the brachial vein to form the axial vein [8]. The vein was simplified as a cylinder of an outer radius of 2.90 mm and a thickness of .50 mm around its circumference. The wound was simplified as a rectangular area at the surface and at the outflow end of the vein. Using these simplifications, the process was modeled as a 3D fluid flow and mass transport problem.

### Process Dynamics

Figure 2 (A - D) shows the process by which P-selectin immunoglobulin is converted to microparticles and then bound to fibrin at the wound site in the basilic vein of hemophiliac patients to speed up their healing process.





**Figures 2 (A - D). Modelled process of the reaction in the blood from the drug.** The project aims to model the use of the drug P-sel-Ig to help form blood clots and to optimize the concentration of well-mixed P-sel-Ig in the blood. The figure above shows the drug P-sel-Ig in the basiliic vein and traveling through the bloodstream (A). P-sel-Ig binds to endothelial cells which produce the protein P-selectin (B). The P-selectin then binds to the receptor on leukocytes in the bloodstream which in turn produce microparticles (C). The microparticles travel to the wound and interact with fibrin proteins in the wound to stimulate fibrogenesis and close up the wound (D). Within this process, microparticles lead to the production of Xa which leads to conversion of prothrombin to thrombin. Thrombin then catalyzes the production of fibrin.

The clotting of the wound through the accumulation of microparticles is modelled through a one way coupling of fluid flow and mass transport. To simplify the problem, it is assumed that P-sel-Ig is well mixed in the circulatory system and that the microparticles have been fully produced at the time at which the wound is made. Thus, the interactions of P-sel-Ig, P-selectin, and leukocytes are all incorporated into the initial concentration of microparticles in the blood stream.

### Design Objectives

The design objectives can be split into the following four goals:

1. Model mass transfer from a well-mixed homogeneous microparticles in a cylindrical vein, so that mass diffusion and timing of fibrin formation are observed
2. Model the reactions that microparticles undergoes to produce a clot, so that the amount of fibrin at the wound can be determined
3. Combine these two processes in COMSOL
4. Use these models to optimize the initial concentration of microparticles to minimize the time for wound healing.

### Governing Equations

The following governing equation (Equation 1) for convection mass transfer will be used to model the transport of microparticles in the basiliic vein:

$$\frac{\partial c_m}{\partial t} + u \cdot \nabla c_m = D \nabla^2 c_m - r_m \quad (1)$$

$$r_m = -K_e c_m \quad (2)$$

Where  $c_m$  is the concentration of microparticles in the blood,  $u$  is the bulk velocity of flow,  $D$  is the diffusivity of microparticles in the blood, and  $(r_m)$  is the reaction constant of microparticles which takes into account the rate at which microparticles are used to produce the clot. The consumption rate of microparticles at the wound is a function of the elimination constant ( $K_e$ ) and the concentration of microparticles ( $c_m$ ) (Equation 2) [13].

The following Navier Stokes equation (Equation 3) and continuity equation (Equation 4) will be used to model transient fluid flow through the basilic vein:

$$\rho(u \cdot \nabla u) = -\nabla P + \mu \nabla^2 u \quad (3)$$

$$\nabla \cdot (\rho u) = 0 \quad (4)$$

Where  $\rho$  is the density of blood,  $u$  is the velocity vector of flow,  $P$  is pressure, and  $\mu$  is the dynamic viscosity (Table 1).

### **Boundary Conditions**

For mass transport of microparticles through the basilic vein, the flux of microparticles will be assumed as negligible at the blood vessel wall compared to the flux of microparticles through the vein. It is also assumed that there is no mass transfer outside of the vein or within the vein wall.

$$r_x = \frac{dX_a}{dt} = \int q_m dA \quad (5)$$

$$r_p = \frac{dP}{dt} = -k_p P X_a \quad (6)$$

$$r_T = \frac{dT}{dt} = k_p P X_a \quad (7)$$

$$r_f = \frac{dF}{dt} = \frac{K_f T}{V_{wound}} \left(1 - \frac{F}{F_{max}}\right) \quad (8)$$

At the wound boundary, microparticle flux ( $q_m$ ) was integrated over the wound area and used to calculate the rate of production of activated Factor X ( $r_x$ ) (Equation 4). The prothrombin consumption rate depends on rate constant ( $k_p$ ), prothrombin concentration ( $P$ ) and activated Factor X concentration (Equation 5). All prothrombin is converted into thrombin (Equation 6). Rate of fibrin polymerization ( $r_f$ ) is characterized by a constant rate  $K_f$  multiplied by the thrombin concentration ( $T$ ) divided by the volume of the wound ( $V_{wound}$ ) (Equation 7).. The ratio of the fibrin concentration ( $F$ ) over the maximum fibrin concentration at the wound ( $F_{max}$ ) accounts for the decreasing rate of fibrin formation as fibrin clots the wound [10].



For fluid flow through the vessel, velocity of the blood at both the surface of the vein and at the wound itself is assumed to be negligible. Furthermore, the inlet velocity of the blood through the basilic vein is simplified as fully developed, laminar parabolic flow with an inlet average velocity of 7.2 cm/s[9]. It is assumed that the outlet pressure of the vein is zero, and there is no slip on all vein walls including the wound.

### **Initial Conditions**

As part of the model, the initial concentration of microparticles in the blood will be varied in order to optimize clotting time based on corresponding P-sel-Ig concentrations. The initial concentration of microparticles in the body, and the initial concentrations of Xa, prothrombin, and thrombin at the wound were approximated using the literature and can be found in Table 1.

### **Results**

After implementing the mesh, the velocity profile in the vessel was computed (Figure 3).

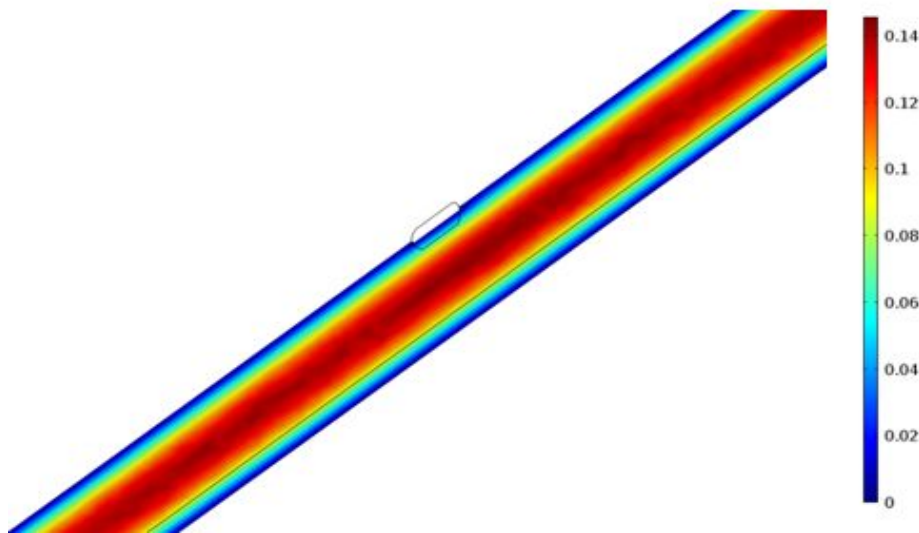


**Figure 3. Cross section velocity profile of the blood vessel.** The color gradient in this figure shows symmetry which indicates parabolic flow.

The acquired velocity profile of the blood vessel showed a parabolic profile with laminar flow. As expected, velocity at the walls of the vessel was zero due to shear stress and was at a maximum at the center of the vessel.

The model was also used to compute surface microparticle concentration distribution in the vessel after the particles were allowed to react at the wound for a period of time (Figure 4).

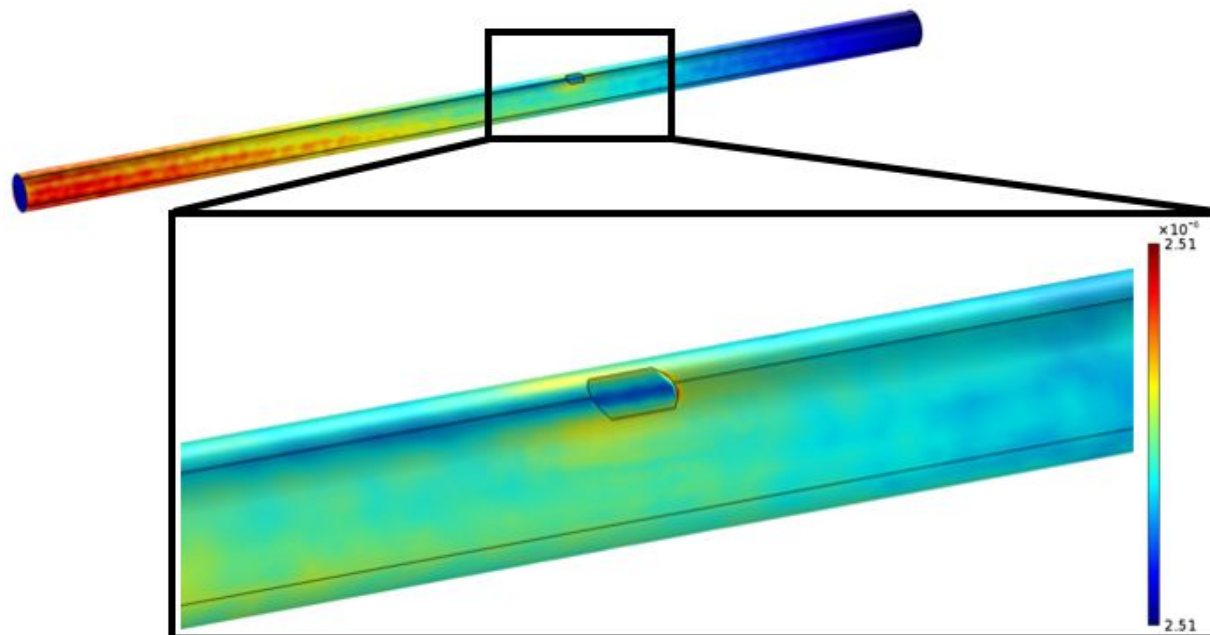


**Figure 4. Surface microparticle concentration distribution.** The concentration profile decreases towards the wound because microparticles are being consumed to aid in the formation of fibrin.

Following clotting time, the concentration profile of the vessel showed a constant level of microparticle at the surface of the vessel and depleted levels at the wound, where microparticles were consumed and reacted to form fibrin, a necessary component of clot formation (Figure 4).

Microparticle body concentration in the vessel as well as Xa concentration and fibrin concentration at the wound were measured over a 3 hour period (Figure 5, 6, 7).

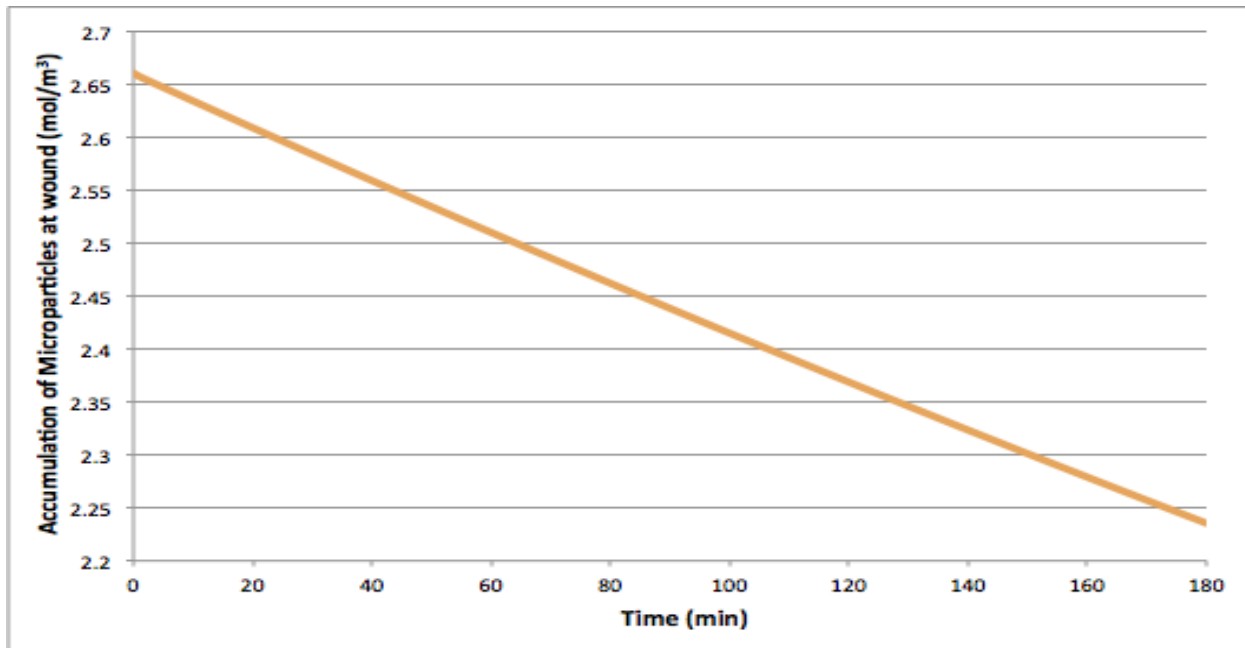


**Figure 5. Microparticle concentration within the domain over time.** This graph depicts microparticles with an initial concentration and no production of microparticles. The concentration decreases slowly because the elimination of the drug within the blood stream is gradual as it cycles through the liver and kidney.

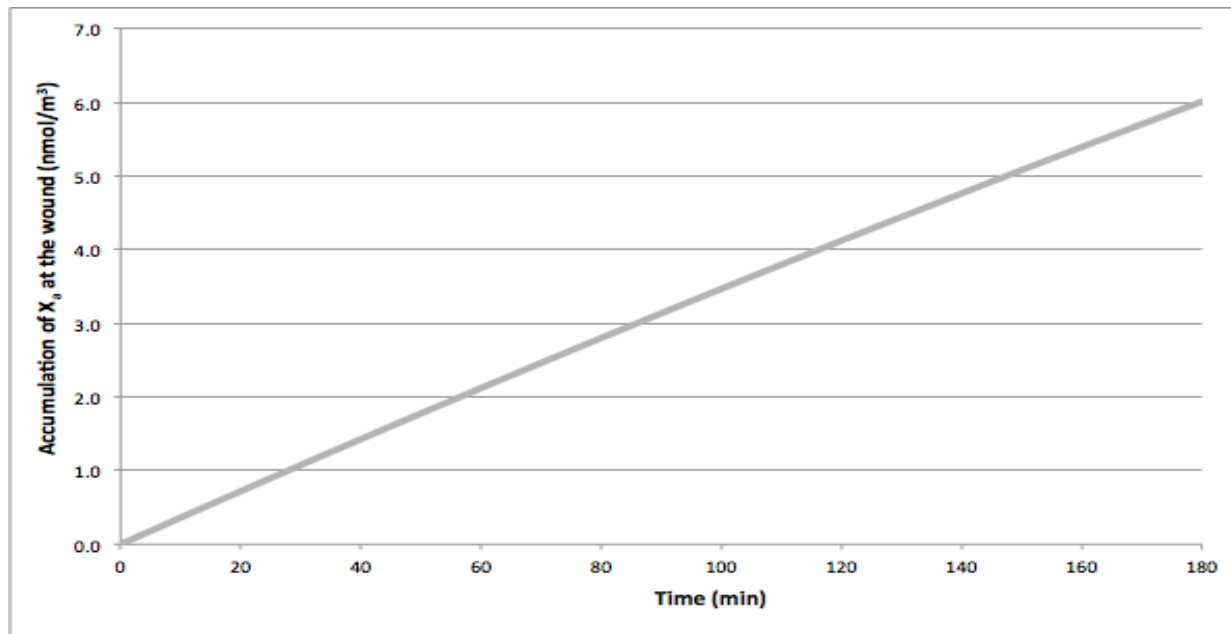


**Figure 6. Concentration of Xa at the wound.** This graph depicts the accumulation of activated Factor X ( $X_a$ ) at the wound. The concentration of Xa increases because microparticles are being consumed. It eventually plateaus, which isn't seen on this graph because it reaches steady state past the time frame set.

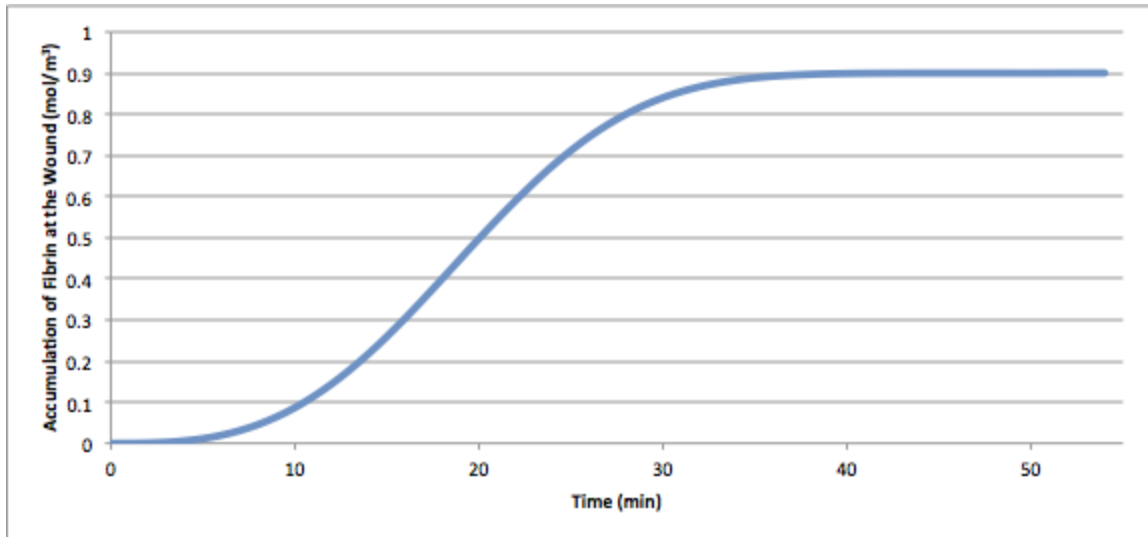


**Figure 7. Concentration of fibrin at the wound.** This graph depicts the accumulation of fibrin at the wound over time. The concentration of fibrin increases because it is activated by  $X_a$ , which is also increasing. Fibrin concentration plateaus because it reaches the maximum fibrin concentration ( $Fib_{max}$ ). The time it plateaus is equivalent to the time it takes for the wound to clot.

Microparticle body concentration fluctuated over the clotting period; initially starting at  $100 \text{ mol/m}^3$ , the body concentration first increased as the dose of P-sel-Ig led to the production of more microparticles. However, as microparticles accumulated in the clot and contributed to clot formation, the body concentration decreased (Figure 5). The corresponding mass of activated Factor X increased at the wound site over time (Figure 6). After a time delay needed for activated Factor X to reach the threshold  $X_t$ , fibrin polymerization began and the mass of fibrin at the wound increased (Figure 7).

### **Sensitivity Analysis**

Using sensitivity analysis, the rate constant parameters and their effect on the solution were observed. Using a parametric sweep in COMSOL, the rate constants (thrombin rate constant and fibrin rate constant) were changed by an order of magnitude in order to observe how the solution changed with respect to the different values (Figure 8, 9). The effects of the two rate constants on the solution were then observed in conjunction with each other (Figure 10).

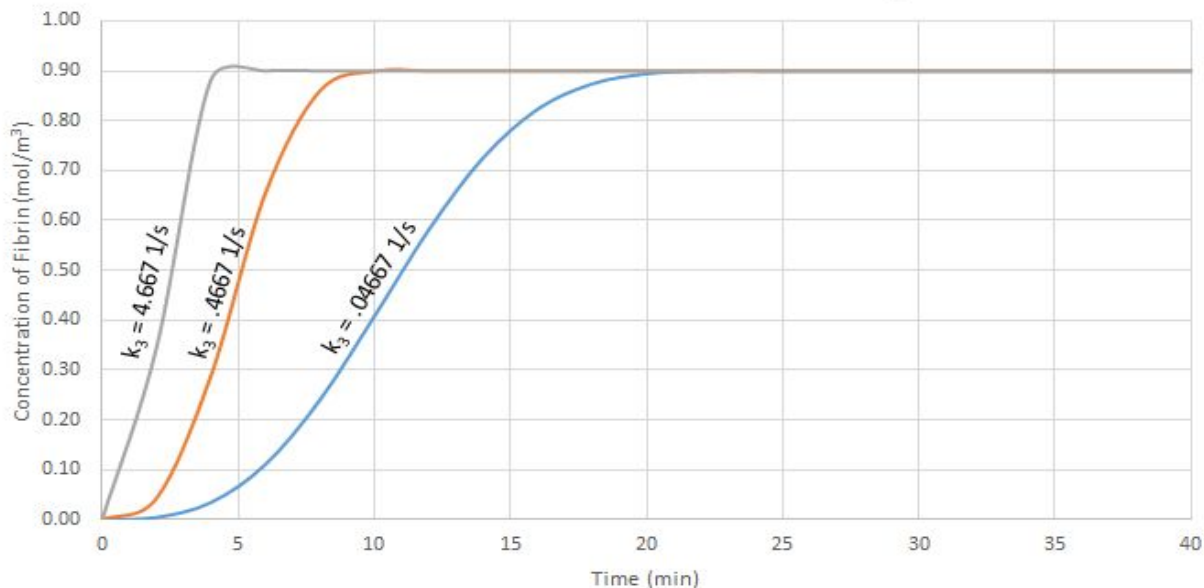


**Figure 8. Fibrin concentration at the wound over different thrombin production rate constants as a function of time.** This graph depicts the sensitivity analysis of the rate of fibrin formation with regards to the rate constant of thrombin production ( $k_3$ ). The values we used to measure the sensitivity of  $k_3$  are a magnitude apart (0.04667, 0.4667, and 4.667 1/s). As the rate of thrombin production increased, the time it took to reach maximum fibrin concentration decreased.

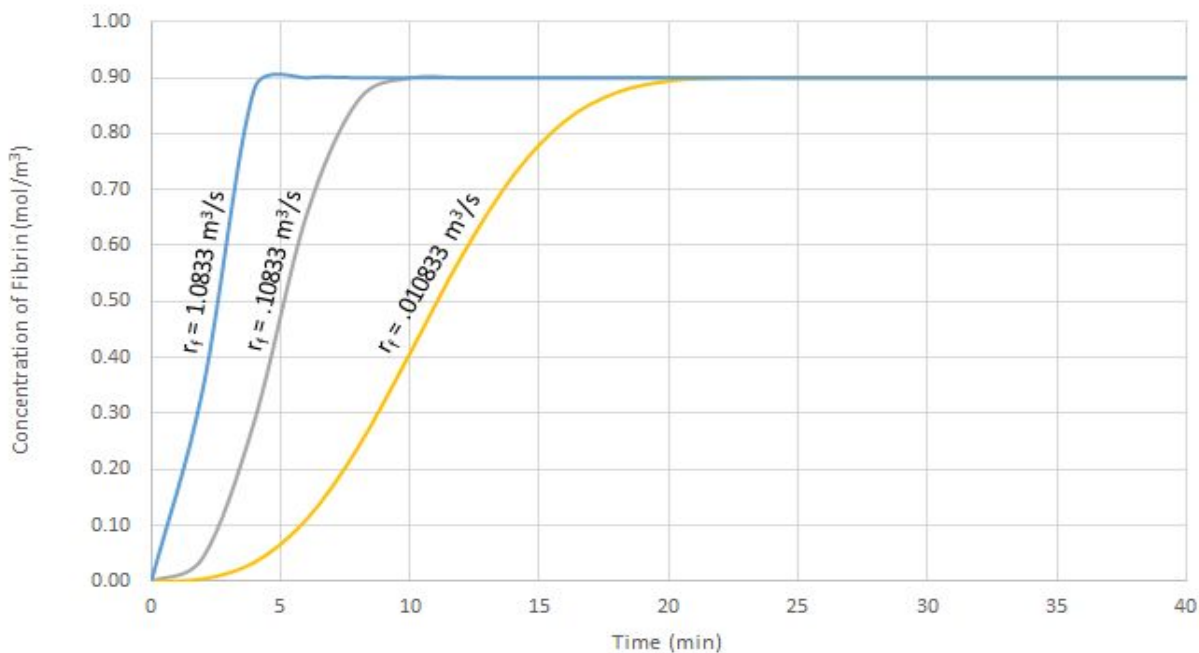


**Figure 9. Fibrin concentration at the wound over different fibrin production rate constants as a function of time.** This graph depicts the sensitivity analysis of the rate of fibrin formation with regards to the rate constant of thrombin production ( $r_f$ ). The values we used to measure the

sensitivity of  $r_f$  are a magnitude apart (0.010833, 0.10833, and 1.0833 1/s). As the rate of fibrin production increased, the time it took to reach maximum fibrin concentration and clot the wound decreased.

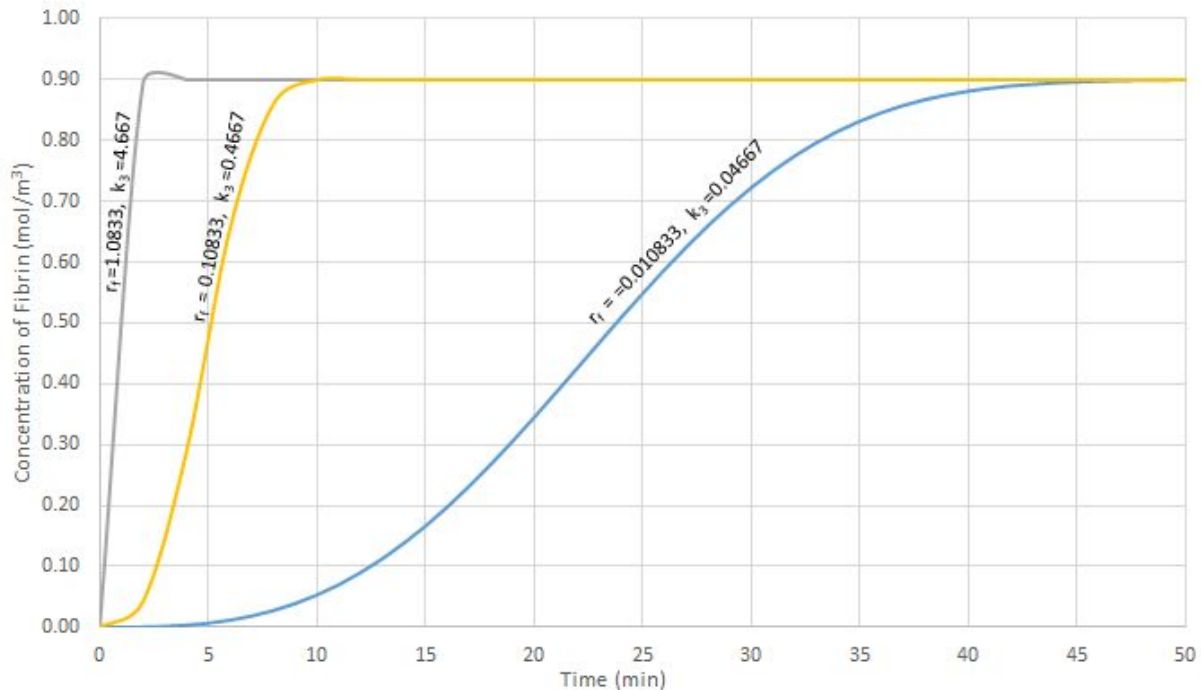


**Figure 10. Fibrin concentration at the wound over different rate constants as a function of time.** This graph depicts the sensitivity analysis of the rate of fibrin formation with regards to the rate constant of thrombin production ( $k_3$ ) and the rate constant of fibrin polymerization ( $r_f$ ). The values we used to measure the sensitivity of  $k_3$  are a magnitude apart (0.04667, 0.4667, and 4.667 1/s) with matching increasing values for  $r_f$  (0.010833, 0.10833, and 1.0833 1/s). The steepest slope and the more gradual slope represent the two extreme combinations of these two rate constants. As the rate of fibrin and thrombin production increased, the time it took to reach maximum fibrin concentration decreased.

By increasing the thrombin rate constant ( $k_3$ ) within a range of possible values in the body, the time at which the blood decreased (Figure 8). Similarly when the fibrin rate constant ( $r_f$ ) was increased by a magnitude of 10, a decrease in the time taken for the wound to clot was observed (Figure 9). When these changes were combined, there was a greater overall impact, resulting in a final clotting time that was within one order of magnitude from the literature (Figure 10) [16]. By using the physiologically relevant clotting time as a reference point, more reasonable rate constants can be determined using this sensitivity analysis.

Sensitivity analysis was also conducted on the initial steady state microparticle concentration in the bloodstream prior to the formation of the wound (Figure 11). Initial microparticle concentration was varied by an order of magnitude.

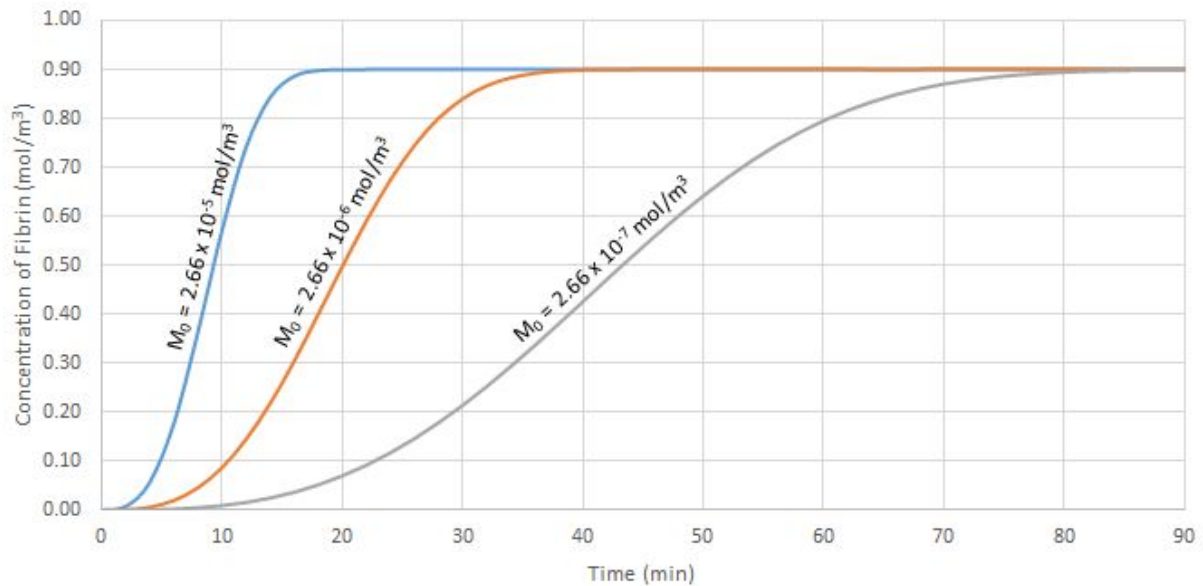


**Figure 11. Fibrin Concentration at the wound over different initial microparticle concentrations as a function of time.** This graph depicts the sensitivity analysis of the rate of fibrin formation with regards to the initial microparticle concentration in the body ( $M_0$ ) prior to wound formation. The values we used to measure the sensitivity of  $M_0$  are a magnitude apart ( $2.66 \times 10^{-7}$ ,  $2.66 \times 10^{-6}$ , and  $2.66 \times 10^{-5}$  mol/m<sup>3</sup>). As the initial microparticle concentration increased, the time it took to reach maximum fibrin concentration decreased.

The analysis showed that as initial circulating microparticle concentration increased, the time it took to reach maximum fibrin concentration at the wound decreased. An increased microparticle concentration correlates with increased tissue factor in the system, which directly contributes to the clotting pathway in humans.

The wound radius was also considered for sensitivity analysis (Figure 12). Wound radius was varied by a factor of two.

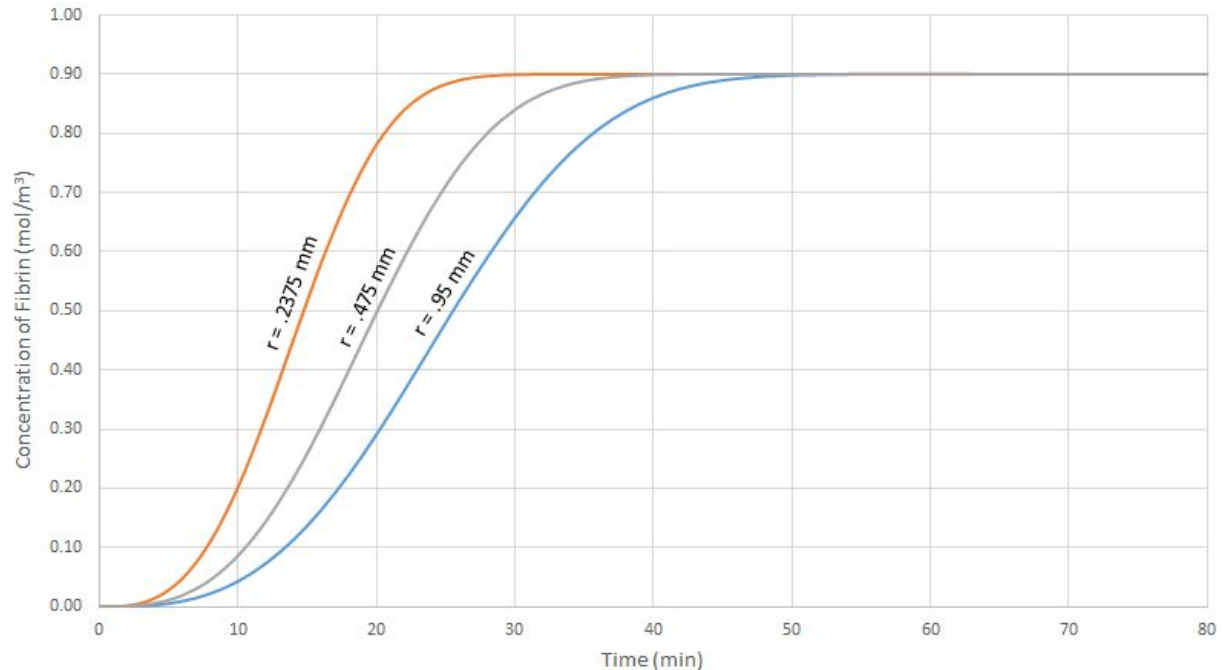


**Figure 12. Fibrin Concentration at the wound over different wound sizes as a function of time.** This graph depicts the sensitivity analysis of the rate of fibrin formation with regards to the radius of the wound ( $r$ ). The values we used to measure the radius of wound are a factor of 2 apart (.2375, .475, and .95 mm). As the size of the wound increased, the time it took to reach maximum fibrin concentration increased. This can be explained in that a larger wound radius would require more fibrin, and with the other parameters staying the same, the time to clot the wound would increase as well.

As expected, as wound size increased, the clotting time subsequently increased.

### Accuracy Check

Physiologically, the average clotting time is approximately 11 minutes in control mice [16]. The model value calculated for time taken to clot the wound in a healthy person is an order of magnitude within this physiological value. This time was obtained by conducting sensitivity analysis (Figure 10) on the thrombin and fibrin production rate constants to achieve a more physiologically accurate value.

### Discussion

The goal of this model was specifically to simulate transport and uptake of microparticles by a wound in the basilic vein in the P-sel-Ig treatment of a Hemophilia A patient using COMSOL. In order to model this process, fluid flow coupled with mass transport of microparticles was considered. Blood flow was modelled as laminar flow. This model also takes into consideration the transformation of microparticles to fibrin. This includes, the activation of Factor X via the



microparticles which facilitates the conversion of prothrombin to thrombin. Then, thrombin catalyzes the production of fibrin, which accumulates at the wound and stops blood loss.

After implementing this model into COMSOL, the velocity profile of the blood in the vessel was obtained. Furthermore, the overall concentration of microparticles in the vessel and the activated factor X and fibrin concentrations at the wound over time were obtained. By relating the fibrin concentration to the maximum fibrin packing constant at the wound, the time necessary to clot the wound was acquired. When all parameters were left at their baseline values (Table 1), it took approximately 35 minutes for the wound to reach a maximum fibrin density ratio of .9 (Figure 7). However, it was determined that for the wound to cease bleeding, only a threshold of about 70% of the max fibrin concentration was needed. It was thus determined that it took approximately 23 minutes for the wound to stop bleeding,

This clotting time was compared to the literature and existing experiments that tested the effectiveness of P-sel-Ig on clotting. A study by Hrachovinová et al., showed that in a mouse exposed to P-sel-Ig 72 hours prior to wound formation, clotting time was approximately 4.5 minutes. This value was within an order of magnitude of our 23 minute clotting time in Hemophilia patients treated with P-sel-Ig, and thus validated our model. This discrepancy can be explained by several sources of interest including inaccurate rate constants, the assumption of a steady state microparticle concentration in the blood, simplification of the reactions at the wound, and differences between mouse and human physiology.

After finding an initial solution to the model sensitivity analysis was conducted on several rate constants, wound size, and initial conditions. As expected, as thrombin and fibrin rate constants increased, the time needed to clot the wound decreased. Sensitivity analysis confirmed that as wound size increased the clotting time also increased. Furthermore, sensitivity analysis was conducted on initial circulating microparticle concentration in the body. As initial microparticle concentration increased, the amount of tissue factor in the system increased and so the clotting time decreased. Using this relation, initial microparticle concentration was able to be optimized to an order of  $10^{-5}$  which results in a clotting time relatively close to that supported by the P-sel-Ig literature.

Future efforts will focus on improving the accuracy of the model by accounting for pulsating blood flow. Future models can also account for Xa and prothrombin free flowing through the vessel for a more accurate depiction of the vessel in a patient. In order to connect the model directly to treating Hemophilia patients an accurate conversion between a P-sel-Ig dose and a circulating microparticle concentration in the bloodstream must be found. Using this conversion, the model can be used to optimize the administered P-sel-Ig dose against clotting time with the hopes of ultimately using it in a patient.

## Appendix

**Table 1.** Constants Used for the Model for Different Parameters

Variable Name	Description	Value with units
$\rho$	Density of blood	1060 kg/m <sup>3</sup>
$\mu$	Dynamic viscosity of blood	0.00278 Pa*s
V	Volume of blood in the body	4.7 L
Thickness	Thickness of vein	0.5 mm
$D_M$	Diffusivity of microparticles	$5.7 \times 10^{12}$ cm <sup>2</sup> /s
$M_0$	Initial microparticle concentration	$2.66 \times 10^{-6}$
$K_e$	Elimination rate of drug in bloodstream	$1.61 \times 10^{-5}$ 1/s
$X_t$	$X_a$ threshold for fibrin polymerization	$1 \times 10^{-7}$ mol/m <sup>3</sup>
$h_m$	Wound absorption of microparticles	$1.14 \times 10^{-10}$ m/s
$k_3$	Rate of thrombin production	0.0077783 1/s
$r_f$	Rate of fibrin production	0.10833 m <sup>3</sup> /s
$Fib_{max}$	Maximum Fibrin	0.9 mol/m <sup>3</sup>

**Table 2.** Variables used within COMSOL

Variable	Description
Xa	Concentration of Xa
Throm	Concentration of Thrombin
bodyC	Concentration of microparticles in the body
ProT	Concentration of Prothrombin
Fib	Concentration of Fibrin

### **Mesh Convergence**

For mesh convergence, the velocity magnitude profile was plotted over the cross section of the vein for extra coarse, coarse, normal, and fine (Figure 13). There was relatively little disparity between the coarse, normal, and fine graphs. However, the visible difference between the extra coarse and coarse graphs indicates the coarse mesh to be preferable over the extra coarse mesh. Specifically, the extra coarse mesh did not follow the definitive parabolic curve indicative of laminar flow as well as the coarse, normal, and fine mesh.

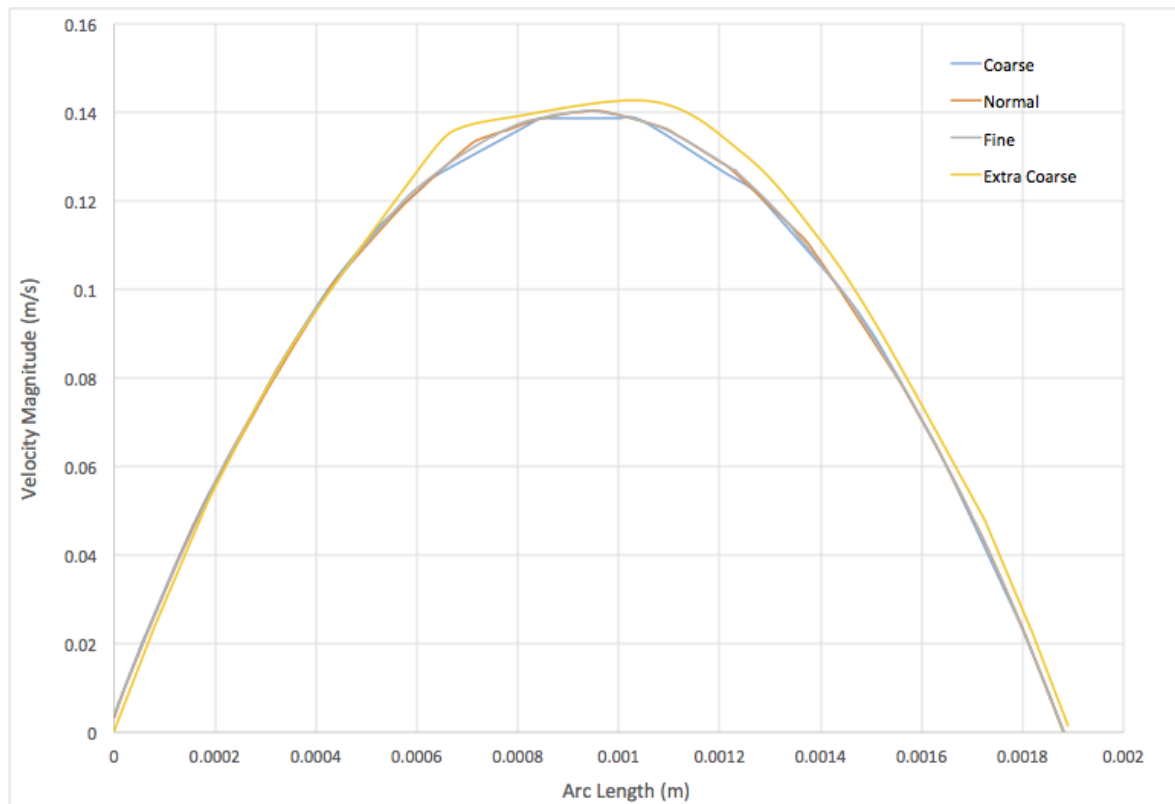


**Figure 13. Concentration of fibrin at the wound with an extra coarse, coarse, normal, and fine mesh.** This graph depicts the accumulation of fibrin at the wound over time in an extra coarse, coarse, normal, and fine mesh defined vessel.

The complete extra coarse mesh consisted of 164,338 domain elements. The complete coarse mesh consisted of 201,972 domain elements. The complete normal mesh consisted of 342,151 domain elements. The fine mesh consisted of 654,592 domain elements. Ultimately, the coarse mesh was used in order to maximize accuracy and minimize computation time.

## References

- [1] Plug, I., Mauser-Bunschoten, E. P., Bröcker-Vriends, A. H., van Amstel, H. K. P., van der Bom, J. G., van Diemen-Homan, J. E., ... & Rosendaal, F. R. (2006). Bleeding in carriers of hemophilia. *Blood*, *108*(1), 52-56.
- [2] Data & Statistics. (2015, July 08). Retrieved March 09, 2016, from <http://www.cdc.gov/ncbddd/hemophilia/data.html>
- [3] Collins, P. W., Hirsch, S., Baglin, T. P., Dolan, G., Hanley, J., Makris, M., ... & UK Haemophilia Centre Doctors' Organisation. (2007). Acquired hemophilia A in the United Kingdom: a 2-year national surveillance study by the United Kingdom Haemophilia Centre Doctors' Organisation. *Blood*, *109*(5), 1870-1877.
- [4] Schwartz, R. S., Abildgaard, C. F., Aledort, L. M., Arkin, S., Bloom, A. L., Brackmann, H. H., ... & Kasper, C. K. (1990). Human recombinant DNA-derived antihemophilic factor (factor VIII) in the treatment of hemophilia A. *New England Journal of Medicine*, *323*(26), 1800-1805.
- [5] Iorio, A., Halimeh, S., Holzhauser, S., Goldenberg, N., Marchesini, E., Marcucci, M., ... & Gringeri, A. (2010). Rate of inhibitor development in previously untreated hemophilia A patients treated with plasma-derived or recombinant factor VIII concentrates: a systematic review. *Journal of Thrombosis and Haemostasis*, *8*(6), 1256-1265.
- [6] Hrachovinová, I., Cambien, B., Hafezi-Moghadam, A., Kappelmayer, J., Camphausen, R. T., Widom, A., ... & Wagner, D. D. (2003). Interaction of P-selectin and PSGL-1 generates microparticles that correct hemostasis in a mouse model of hemophilia A. *Nature medicine*, *9*(8), 1020-1025.
- [7] Basilic Vein. (2015). Retrieved March 09, 2016, from [https://www.innerbody.com/image\\_cardov/card23-new.html](https://www.innerbody.com/image_cardov/card23-new.html)
- [8] Baptista-Silva, J. C. C., Dias, A. L., Cricenti, S. V., & Burihan, E. (2003). Anatomy of the basilic vein in the arm and its importance for surgery. *Braz J Morphol Sci*, *20*(3), 171-175.
- [9] Ooue, A., Ichinose-Kuwahara, T., Shamsuddin, A. K. M., Inoue, Y., Nishiyasu, T., Koga, S., & Kondo, N. (2007). Changes in blood flow in a conduit artery and superficial vein of the upper arm during passive heating in humans. *European journal of applied physiology*, *101*(1), 97-103.
- [10] Zubairova, L. D., Nabiullina, R. M., Nagaswami, C., Zuev, Y. F., Mustafin, I. G., Litvinov, R. I., & Weisel, J. W. (2015). Circulating Microparticles Alter Formation, Structure, and Properties of Fibrin Clots. *Scientific reports*, *5*.
- [11] Ay, C., Jungbauer, L. V., Sailer, T., Tengler, T., Koder, S., Kaider, A., ... & Mannhalter, C. (2007). High concentrations of soluble P-selectin are associated with risk of venous thromboembolism and the P-selectin Thr715 variant. *Clinical chemistry*, *53*(7), 1235-1243.

- [12] Pereira, V. D., & Campos Silva, J. B. (2005). Simulations of incompressible fluid flows by a least squares finite element method. *Journal of the Brazilian Society of Mechanical Sciences and Engineering*, 27(3), 274-282.
- [13] Al-Qallaf, B., Das, D. B., Mori, D., & Cui, Z. (2007). Modelling transdermal delivery of high molecular weight drugs from microneedle systems. *Philosophical Transactions of the Royal Society of London A: Mathematical, Physical and Engineering Sciences*, 365(1861), 2951-2967.
- [14] Celi, A., Lorenzet, R., Furie, B. C., & Furie, B. (2004). Microparticles and a P-selectin-mediated pathway of blood coagulation. *Disease Markers*, 20, 347-352.
- [15] Wood, J. P., Silveira, J. R., Maille, N. M., Haynes, L. M., & Tracy, P. B. (2011). Prothrombin activation on the activated platelet surface optimizes expression of procoagulant activity. *Blood*, 117(5), 1710–1718.  
<http://doi.org/10.1182/blood-2010-09-311035>
- [16] Polgar, J., Matuskova, J., & Wagner, D. D. (2005). The P-selectin, tissue factor, coagulation triad. *Journal of Thrombosis and Haemostasis*, 3(8), 1590-1596.